

## Dependence of Energy Source Properties of Tube Cathode Arc on Cathode Shape

T. Tamaki, S. Tashiro, M. Tanaka, M. Nakatani\* and Y. Yamazaki\*

Joining and Welding Research Institute, Osaka University, 11-1 Mihogaoka, Ibaraki, Osaka 576-0047

e-mail: tamaki@jwri.osaka-u.ac.jp

\* Hitachi Zosen Corporation, 2-11, Funamachi 2-chome, Taisho-ku, Osaka 551-0022

A plasma torch can stabilize high temperature arc plasma by employing shielding gas and has high heating efficiency and highly controllable characteristics. Therefore, it is widely utilized as a heat source device, for example, for production of nano-particles, material processing, or treatment of toxic waste and so on. Tube Cathode Arc (TCA) is a kind of plasma torch which produces the arc plasma by introducing the shielding gas from the hole of the tube cathode. It has been studied as a heat source especially in lower pressure environment, for example, for space welding or plasma CVD. For an application in atmospheric pressure, it enables heating of materials uniformly and, therefore, to be suitable for processes such as thermal spraying, brazing or buildup. In this paper, as basic energy source properties of argon TCA, dependence of the arc plasma property on cathode shapes such as diameter and conical angle of the cathode are numerically analyzed.

Key words: Energy Source Property, Tube Cathode Arc, Cathode Shape

### 1. INTRODUCTION

Since a plasma torch can stabilize high temperature arc plasma by employing shielding gas, it is generally used as a heat source device. Gas Tungsten Arc (GTA) is the most widely employed type of the plasma torch and produces the arc plasma between a tungsten cathode and an anode material. It has high heating efficiency and highly controllable characteristics, and requires low cost for equipment investment. Furthermore, the target material can be heated without any chemical reaction by using inert gas as the shielding gas. Therefore, it is widely utilized, for example, for production of nano-particles, material processing such as melting, cutting and welding [1], or decomposition, volume reduction and detoxification of toxic waste [2] and so on.

Since the arc current is originated mainly from thermionic emission of electrons on the high temperature cathode surface, it is significantly important to control the temperature distribution on the cathode surface to realize the required properties of the arc plasma and improve its stability. The cathode temperature is determined by energy balance between heating and cooling processes such as ion collision, heat transfer, joule heating, radiation, thermionic emission of electrons and water cooling etc [3]. The energy balance strongly depends on the cathode shape [4]. In the case of GTA, the arc current is concentrated at a point on the tip of the cathode because of the conical cathode shape. It leads to the constriction of the arc plasma and, hence, enables to produce the arc plasma with high energy density and realizes high stability of arc plasma due to large amount of thermionic emission of electrons caused by the high temperature cathode surface [5]. Therefore, GTA is suitable especially for processes which require concentrating the heat intensity at a point but less effective for processes which require

heating the target material uniformly.

On the other hand, Hollow Cathode Arc (HCA) is a kind of GTA which produces the arc plasma by introducing the shielding gas through a central hole of the hollow cathode. It has been studied as the heat source especially in lower pressure, for example, for space welding [6] or plasma CVD [7], because it is suitable to supply the shielding gas in the electrode gap. Recently, the basic heat source properties of argon (Ar) HCA at atmospheric pressure was numerically analyzed and it was revealed that a large volume of uniform high temperature plasma is produced by adjusting flow rate of the shielding gas introduced through the central hole of the hollow cathode [8]. It is expected that this characteristics is suitable for thermal spraying [9]. In this case, since the target material such as powder is injected through the hollow cathode into the high temperature arc plasma near the cathode directly, it can be heated more efficiently and uniformly. Furthermore it was also found that heat intensity and arc pressure onto the anode surface decrease compared with those of conventional GTA. It is considered that the lower heat intensity makes possible to preserve anode material from damage due to excessive heat intensity during the process and, therefore, it is suitable for processes such as brazing or buildup. In addition, it is also expected that the lower arc pressure enables to realize high-speed welding. However, the heat source properties of HCA at the atmospheric pressure are not fully understood.

In this paper, HCA at atmospheric pressure is termed as Tube Cathode Arc (TCA), because the mechanism of electron emission is different from that in low pressure. The basic heat source properties of Ar TCA for various cathode shapes such as diameter and conical angle of the cathode are numerically analyzed.

## 2. SIMULATION MODEL

The tungsten cathode, the arc plasma and the water-cooled copper anode are described in a frame of cylindrical coordinate with axial symmetry around the arc axis. The calculation domain is shown in Figure 1. The inner diameter of the cathode  $\phi_i$  is 1.0 mm and the outer diameter of the cathode  $\phi_o$  is set to be 1.6, 2.4 or 3.2 mm. The conical angle of the cathode  $\theta$  is set to be 30 or 60 deg. The electrode gap is 5 mm. The arc current of 200 A is given inside the cathode on the upper boundary. Ar is introduced at the flow rate of 10 L/min. from the outside of the cathode on the upper boundary. Furthermore, at the flow rate of 0.5 L/min. an inner shielding gas is additionally introduced through the hole of the tube cathode. The flow is assumed to be laminar, and the arc plasma is assumed to be under the local thermodynamic equilibrium (LTE). Azimuthally uniform expansion of the cathode spot is also assumed. The other numerical modeling methods are given in detail in our previous papers [3, 5]. The differential equations (1)-(6) are solved iteratively by the SIMPLEC numerical procedure [10]:

Mass continuity equation;

$$\frac{1}{r} \frac{\partial}{\partial r} (r \rho v_r) + \frac{\partial}{\partial z} (\rho v_z) = 0 \quad (1)$$

Radial momentum conservation equation;

$$\begin{aligned} \frac{1}{r} \frac{\partial}{\partial r} (r \rho v_r^2) + \frac{\partial}{\partial z} (\rho v_r v_z) = -\frac{\partial P}{\partial r} - j_z B_\theta + \frac{1}{r} \frac{\partial}{\partial r} \left( 2r\eta \frac{\partial v_r}{\partial r} \right) \\ + \frac{\partial}{\partial z} \left( \eta \frac{\partial v_r}{\partial z} + \eta \frac{\partial v_z}{\partial r} \right) - 2\eta \frac{v_r}{r^2} \end{aligned} \quad (2)$$

Axial momentum conservation equation;

$$\begin{aligned} \frac{1}{r} \frac{\partial}{\partial r} (r \rho v_r v_z) + \frac{\partial}{\partial z} (\rho v_z^2) = -\frac{\partial P}{\partial z} + j_r B_\theta + \frac{\partial}{\partial z} \left( 2r\eta \frac{\partial v_z}{\partial z} \right) \\ + \frac{1}{r} \frac{\partial}{\partial r} \left( r\eta \frac{\partial v_r}{\partial z} + r\eta \frac{\partial v_z}{\partial r} \right) \end{aligned} \quad (3)$$

Energy conservation equation;

$$\begin{aligned} \frac{1}{r} \frac{\partial}{\partial r} (r \rho v_r h) + \frac{\partial}{\partial z} (\rho v_z h) = \frac{1}{r} \frac{\partial}{\partial r} \left( \frac{r\kappa}{c_p} \frac{\partial h}{\partial r} \right) + \frac{\partial}{\partial z} \left( \frac{\kappa}{c_p} \frac{\partial h}{\partial z} \right) \\ + j_r E_r + j_z E_z - R \end{aligned} \quad (4)$$

Current continuity equation;

$$\frac{1}{r} \frac{\partial}{\partial r} (r j_r) + \frac{\partial}{\partial z} (j_z) = 0 \quad (5)$$

Ohm's law;

$$j_r = -\sigma E_r, j_z = -\sigma E_z \quad (6)$$

where  $t$  is time,  $h$  is enthalpy,  $P$  is pressure,  $v_z$  and  $v_r$  are the axial and radial velocities,  $j_z$  and  $j_r$  are the axial and radial component of the current density,  $g$  is the acceleration due to gravity,  $\kappa$  is the thermal conductivity,  $C_p$  is the specific heat,  $\rho$  is the density,  $\eta$  is the viscosity,  $\sigma$  is the electrical conductivity,  $R$  is the radiation emission coefficient,  $E_r$  and  $E_z$  are the radial and axial

components of the electric field defined by  $E_r = -\partial V / \partial r$  and  $E_z = -\partial V / \partial z$ , respectively, where  $V$  is electric potential. The azimuthal magnetic field  $B_\theta$  induced by the arc current is evaluated by maxwell's equation.

$$\frac{1}{r} \frac{\partial}{\partial r} (r B_\theta) = \mu_0 j_z \quad (7)$$

where  $\mu_0$  is the permeability of free space.

In the solution of Eqs. (1)-(6), special account needs to be taken at the electrode surface for effects of energy that only occur at the surface. At the cathode surface, additional energy flux terms need to be included in Eq. (4) for thermionic cooling due to the emission of electrons, ion heating, and radiation cooling. The additional energy flux for the cathode  $H_K$  is:

$$H_K = -\epsilon \alpha T^4 - |j_e| \phi_K + |j_i| V_i \quad (8)$$

where  $\epsilon$  is the surface emissivity,  $\alpha$  is the Stefan-Boltzmann constant,  $\phi_K$  is the work function of the tungsten cathode,  $V_i$  is the ionization potential of argon,  $j_e$  is the electron current density, and  $j_i$  is the ion current density. At the cathode surface, for thermionic emission of electrons,  $j_e$  cannot exceed the Richardson current density  $J_R$  [11] given by:

$$|j_R| = AT^2 \exp \left( -\frac{e\phi_e}{k_B T} \right) \quad (9)$$

where  $A$  is the thermionic emission constant for the cathode surface,  $\phi_e$  is the effective work function for thermionic emission of the electrode surface at the local surface temperature, and  $k_B$  is the Boltzmann's constant. The ion-current density  $j_i$  is then assumed to be  $|j| - |j_R|$  if  $|j|$  is greater than  $|j_R|$ ; where  $|j| = |j_e| + |j_i|$  is the total current density at the cathode surface obtained from Eq. (5)

Similarly, for the anode surface, Eq. (4) needs additional energy flux terms for thermionic heating and radiation cooling. The additional energy flux for the anode  $H_A$  is:

$$H_A = -\epsilon \alpha T^4 + |j| \phi_A \quad (10)$$

where  $\phi_A$  is the work function of the anode and  $|j|$  is the current density at the anode surface obtained from Eq. (5). The term including  $\phi_A$  accounts for the heating of the anode by electrons, which delivers energy equal to the work function on being absorbed at the anode. The term is analogous to the cooling effect that occurs at the cathode when electrons are emitted.

## 3. RESULTS AND DISCUSSION

Figures 2-4 show two-dimensional distribution of temperature and fluid flow velocity for  $\theta=60$  deg. and  $\phi_o=1.6, 2.4$  and 3.2 mm, respectively. It was found that maximum plasma temperature near the cathode tip increases with decrease of  $\phi_o$ . It is considered that current density in the arc plasma near the cathode tip increases because expansion of current distribution in

radial direction is restricted by  $\phi_0$  and it leads to an increase in Joule heat. Furthermore, since cathode jet is accelerated due to enhanced electromagnetic pinch force caused by high current density, high temperature region in the arc plasma produced near the cathode tip expands towards the anode. It promotes heat intensity onto the anode and raises the anode temperature. On the other hand, Figure 5 shows result for  $\theta=30$  deg. and  $\phi_0=2.4$  mm. It is seen that maximum plasma temperature and cathode jet velocity are approximately comparable with result shown in Fig. 3 and variation in  $\theta$  hardly affects property of arc plasma.

Figure 6 shows axial distributions of cathode temperature. It is obvious that the cathode tip temperature rises with decrease in  $\phi_0$ . One reason to account for this is due to the effect of Joule heat in the cathode and thermal conduction from high temperature arc plasma near the cathode tip. Similarly, the cathode temperature rises with decrease in  $\theta$  due to Joule heat in the cathode especially near the tip.

Figures 7 and 8 show radial distributions of heat intensity and arc pressure onto anode surface, respectively. It was revealed that heat intensity and arc pressure increase with decrease in  $\phi_0$ . This is because the cathode jet velocity becomes faster inversely proportional to  $\phi_0$ . It leads to increase in arc pressure. In addition, heat intensity also increases due to greater thermal conduction onto the anode surface caused by the expansion of high temperature region in the arc plasma towards the anode. It is also seen that the dependence of heat intensity and arc pressure on  $\theta$  is negligible, since the property of the arc plasma is hardly affected by  $\theta$ .

The increase in the cathode temperature promotes thermionic electron emission from the cathode surface required for supplying the arc current and, consequently, improves the stability of the arc plasma. As a result, small  $\phi_0$  increases not only the cathode temperature but also heat intensity and arc pressure. On the other hand, small  $\theta$  lifts the cathode temperature and stabilizes the arc plasma maintaining low heat intensity and arc pressure.

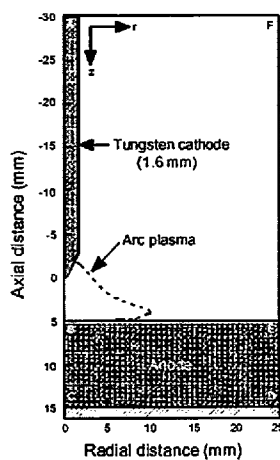


Fig. 1. Schematic illustration of simulation domain.

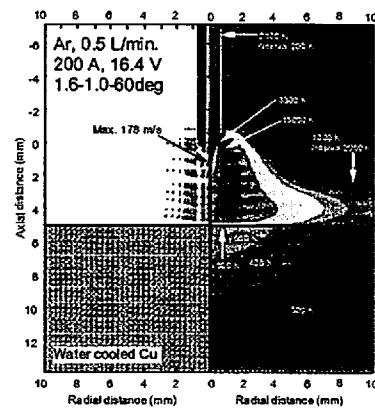


Fig. 2. Two-dimensional distribution of temperature and fluid flow velocity for  $\phi_0 = 1.6$  mm and  $\theta = 60$  deg.

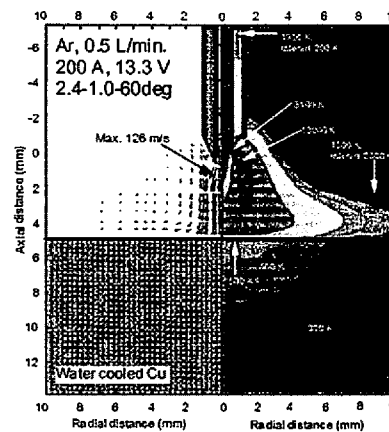


Fig. 3. Two-dimensional distribution of temperature and fluid flow velocity for  $\phi_0 = 2.4$  mm and  $\theta = 60$  deg.

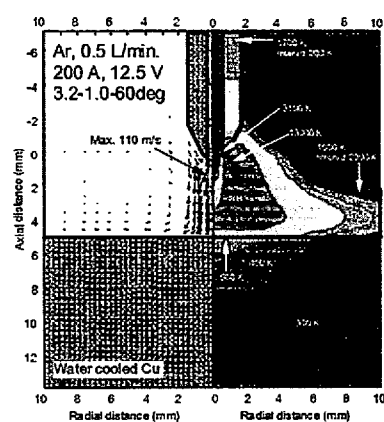


Fig. 4. Two-dimensional distribution of temperature and fluid flow velocity for  $\phi_0 = 3.2$  mm and  $\theta = 60$  deg.

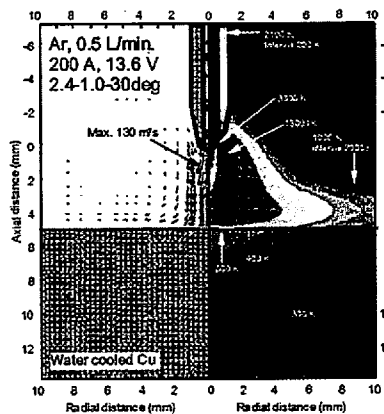


Fig. 5. Two-dimensional distribution of temperature and fluid flow velocity for  $\phi = 2.4 \text{ mm}$  and  $\theta = 30 \text{ deg}$ .

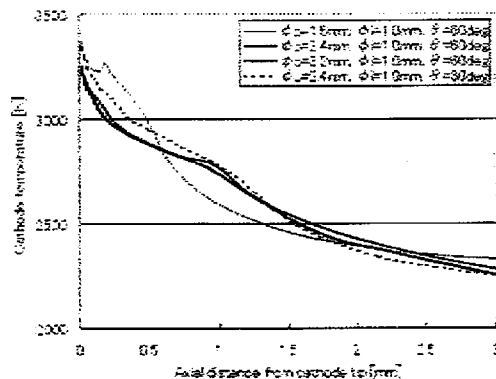


Fig. 6. Axial distributions of cathode temperature.

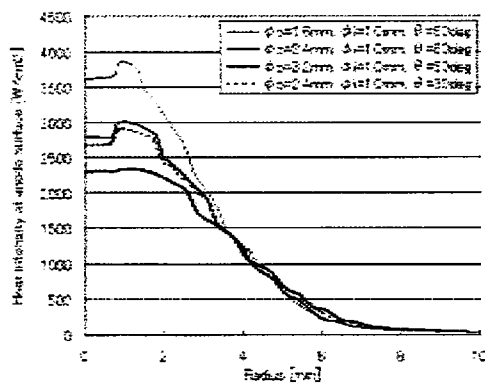


Fig. 7. Radial distributions of heat intensity at anode surface.

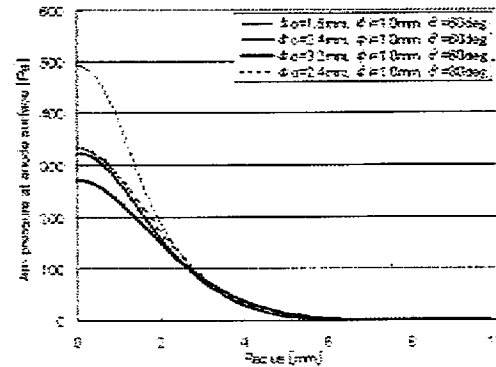


Fig. 8. Radial distributions of arc pressure at anode surface.

#### 4. CONCLUSIONS

The basic heat source properties of Ar TCA for various cathode shapes such as diameter and conical angle of the cathode were numerically analyzed. The main conclusions are summarized as follows:

- 1) Small  $\phi$  restricted expansion of arc current in radial direction and increased current density. It led to increase of not only the cathode temperature but also heat intensity and arc pressure.
- 2) Small  $\theta$  lifted the cathode temperature and stabilized the arc plasma thus maintaining low heat intensity and arc pressure.

#### References

- [1] M. Ushio, et.al., *IEEE Trans. P. S.*, **32**, 108 (2004).
- [2] T. Inaba, et.al., *IEEE Trans. D. E. I*, **7**, 684 (2000).
- [3] M. Tanaka, et.al., *Vacuum*, **73**, 381 (2004).
- [4] J. Haidar and A. J. D. Farmer, *J. Phys. D: Appl. Phys.*, **27**, 555-560 (1994).
- [5] M. Tanaka, et.al., *Plasma Chem. Plasma Process*, **23**, 585-606 (2003).
- [6] Y. Suita, et.al., *Welding Int.*, **8-4** (1994), 269
- [7] G.F.Zhang et.al., *Diamond related materials*, **8**, 2148-2151 (1999).
- [8] S. Tashiro, et.al., *Trans. MRS-J*, **31**, 483- 486 (2006).
- [9] C.-J. Ki and B. Sun, *Thin Solid Films*, **450**, 282 (2004).
- [10] S. V. Patanker, "Numerical heat transfer and fluid flow" Washington DC, Hemisphere Publishing Corporation, 1980
- [11] E. Pfender, "Electric Arcs and Arc Gas heaters, Ch. 6", published in M. H. Hirsh and H. J. Oskam, *Gaseous Electronics*, Academic Press, NewYork (1978) 291-398.

(Received December 9, 2006; Accepted February 28, 2007)